Study on Properties of LBW Joint of AISI 304 Pipes Used in Nuclear Power Plant

Jingyao Chen, Xiao Wei, Jijin Xu, Yi Duan, Junmei Chen, Chun Yu and Hao Lu

Abstract In this work, a girth weld of AISI 304 stainless steel pipes with a dimension of Φ89 mm × 250 mm × 14.5 mm was produced by laser beam welding. The microstructure was observed by optical microscopy. The microhardness test was carried out to study the mechanical properties of the welded joint. A slow strain rate test was performed to investigate the susceptibility to stress corrosion cracking (SCC) of the welded joint in the simulated pressurized water reactor environment. The results show that the values of microhardness in the weld and HAZ are close to those in the parent material. According to ultimate tensile strength-loss rate, elongation-loss rate and fractograph analysis, the welded joint has low susceptibility to SCC in the simulated pressurized water reactor environment.

Keywords Laser beam welding · Slow strain rate test · SCC susceptibility Microhardness · AISI 304 stainless steel

1 Introduction

AISI 304 austenitic stainless steel has been widely used in the fabrication industries including nuclear power industry because of its excellent weldability, good mechanical characteristics and corrosion resistance properties [1]. It is a significant structural material of the pressurized water reactor, which is commonly fabricated by welding techniques.

J. Chen · X. Wei · J. Xu (✉) · Y. Duan · J. Chen (✉) · C. Yu · H. Lu
Key Lab of Shanghai Laser Manufacturing and Materials Modification,
School of Materials Science and Engineering, Shanghai Jiao Tong University,
200240 Shanghai, China
e-mail: xujijin_1979@sjtu.edu.cn

J. Chen
e-mail: chenjm@sjtu.edu.cn

© Springer Nature Singapore Pte Ltd. 2018

S. Chen et al. (eds.), *Transactions on Intelligent Welding Manufacturing*,
Transactions on Intelligent Welding Manufacturing,
https://doi.org/10.1007/978-981-10-8330-3_10

Laser beam welding (LBW), as a new welding technology, is widely developed and applied in many manufacturing industries due to its excellent properties including low heat input, small heat affected zone, high producing efficiency and deep penetration. However, welding leads to low mechanical properties owing to the metallurgical changes during the welding process [2, 3], which will affect the performances of welded structures in services, such as the occurrence of stress corrosion cracking (SCC).

SCC can lead to accidents during the long-term services, which has become a serious problem in the nuclear power industry [4]. The SCC initiates and grows near the welding zone because of high tensile residual stress by welding same as the other contributing factors of material and environment [5]. It is caused and accelerated by the presence of corrosive environments, residual stress, and material sensitization effects [6]. Plenty of researches [7, 8] have been reported to study the SCC behavior of stainless steel in corrosive environment.

Slow strain rate test (SSRT) is a widely used method on stress corrosion cracking researches as the basic experimental technique to promote the incidences of cracking and assess the ranking of susceptibility of different alloys in several corrosive environments. However, few research which focused on the SCC behavior of thick pipeline joints induced by LBW was reported.

In this work, a girth weld of AISI 304 stainless steel thick pipes was produced by LBW. The microstructure of joint was observed by optical microscopy. The microhardness test was carried out to study the mechanical properties of the joint. A slow strain rate test was performed to investigate the susceptibility to SCC of the welded joint in the simulated pressurized water reactor environment.

2 Experimental Procedures

2.1 Materials and Welding Process

The dimension of AISI 304 pipes is Φ89 mm $\times$ 250 mm $\times$ 14.5 mm. The composition of parent material was shown in Table 1. Table 2 shows the welding parameters. During welding, temperature histories were recorded with thermocouples located on the inner surface of pipe, 4 mm to the weld center. After Welding, the axial shrinkage was measured based on fixed point method.

After polished by emery paper, the specimen was electrolytic etched by oxalic acid, which are composed of 10 g oxalic and 90 g distilled water. Afterwards, the microstructures of the joint were captured by an optical microscope.

Table 1 Chemical compositions of parent metal and filler (wt%)

Materials	C	Mn	Cr	S	Ni	Si	P	Fe
304	0.06	1.89	18.67	0.014	8.53	0.42	0.032	other

Table 2 The welding parameters

Methods	Groove type	Weld pass	Power	Rate	Shield gas
LBW	I-type	Single-pass	11 kW	8 mm/s	N_2

2.2 *Microhardness Test*

The microhardness of the joint was measured by Zwick automatic hardness tester in the longitudinal direction. Each test point was evaluated with a testing load of 300 g and was measured with an interval of 0.5 mm.

2.3 *Slow Strain Rate Test*

Rod like samples were sliced from welded pipelines along the longitudinal direction and ensure the weld metal at the center of specimens. The gauge length is 25.4 mm and the gauge diameter is 4 mm.

The SCC susceptibility of the joints was studied by SSRT with a strain rate of 4×10^{-7}/s in a simulated primary water environment at 350 °C and 11.5 MPa without dissolved oxygen. The simulated primary water contained 1200 ppm B as boric acid and 2.2 ppm Li as lithium hydroxide. The fractography of specimens after fracture was characterized by JSM-7800F scanning electron microscope (SEM).

3 Results and Discussion

3.1 *Microstructure*

Macroscopic cross-section of the specimen and the microstructure of different regions, including weld metal (WM), fusion zone (FZ), heat affected zone (HAZ) and parent metal (PM) in the joint, are shown in Fig. 1. The joint shows no cracks and porosities from Fig. 1a. It shows narrow weld width and small fusion area due to high welding speed and low heat input during welding process. The fusion area is 57.61 mm^2. The axial shrinkage of the joint can be calculated by the empirical formula as follows:

$$\Delta y = 0.2\frac{A_H}{\delta} \tag{1}$$

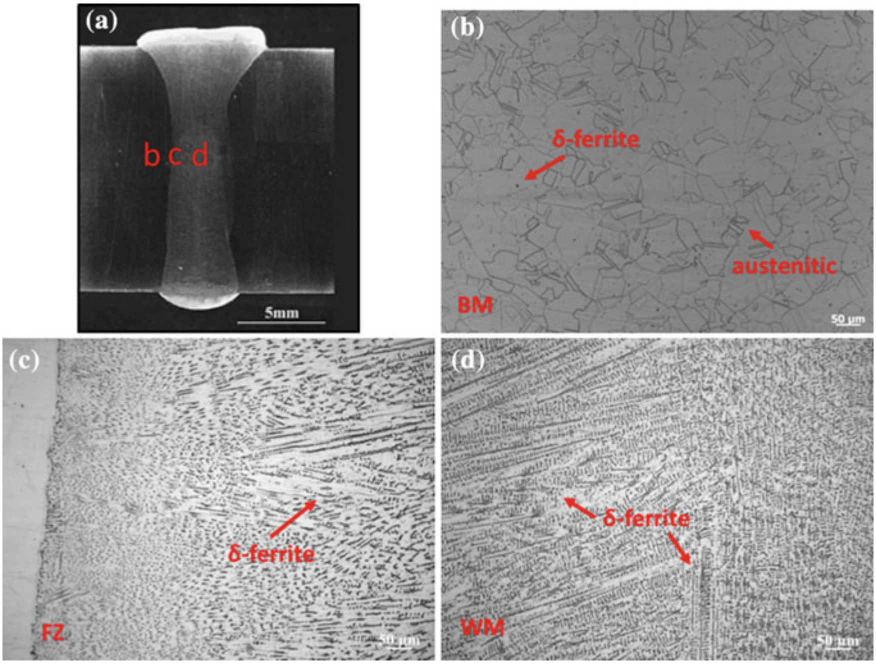

Fig. 1 Microstructure of **a** Overview **b** BM **c** FZ **d** WM

Δy is the axial shrinkage; A_H is the fusion area and δ is the thickness of the pipes. The calculated axial shrinkage of the joint is 0.79 mm, which is close to the measured value, 0.56 mm [9].

According to Fig. 1b–d, the parent metal of AISI 304 stainless steel is composed of equiaxed austenitic grains and a small volume fraction of δ-ferrite. While the weld metal of the joint is composed of austenitic matrixes and plenty of δ-ferrite dendrites, which means that lots of δ-ferrite produced during welding process remained. The solidification process in welding is a non-equilibrium and fast process and the temperature in fusion zone is higher than the temperature of phase balance between δ-Fe and γ-Fe phase so that a lot of δ-ferrite occurred in joint [10]. The dendrites grow from weld metal to fusion line because the direction of grain growth is the opposite to the direction of heat dissipation.

3.2 Microhardness

The microhardness of the joint was measured along the transverse direction parallel to the surface. The results were shown in Fig. 2. Temperature histories during welding are presented in Fig. 3.

Fig. 2 Distribution of hardness in longitudinal direction

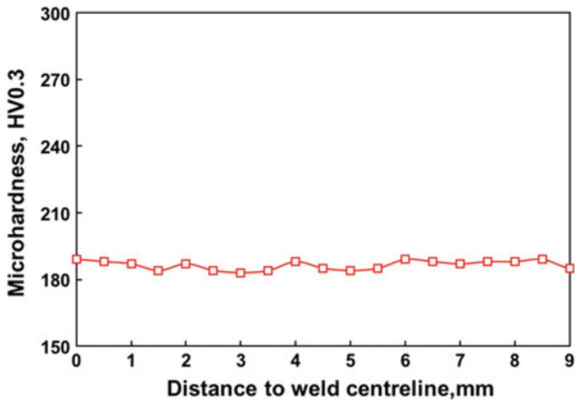

Fig. 3 Welding thermal cycle of the measured point of the joint

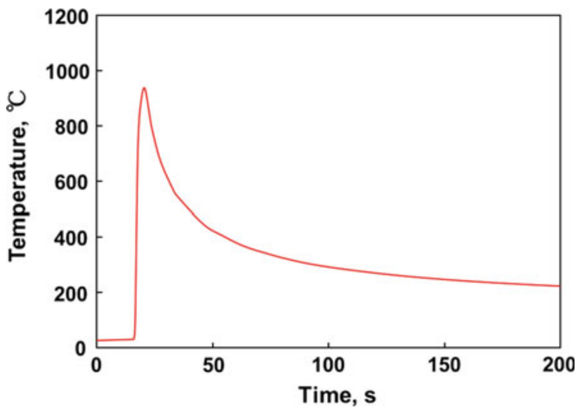

From Fig. 2, it is observed that microhardness changes little along the transverse direction and the values of weld metal and HAZ were close to the hardness of parent metal. The $t_{8/5}$ of the measured point is about 16 s according to Fig. 3. The cooling time of the joint from 800 to 500 °C is larger than usual because of the thickness of the pipes and it reveals higher heat input during welding process which results in similar microhardness in weld metal and parent metal.

3.3 SSRT

3.3.1 Stress-Strain Curves

The stress-strain curves of the SSRT are presented in Fig. 4. The results show that the yield strength and ultimate tensile strength in water environment are lower than the tensile properties in air condition. The tensile properties depression of the joint

Fig. 4 Stress-strain curves of joint during SSRT

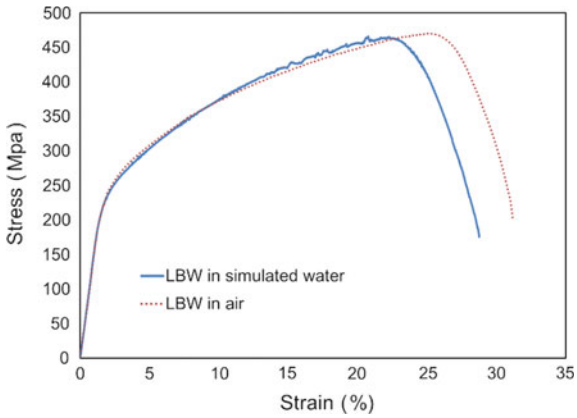

shows SCC characteristics. Generally, ultimate tensile strength-loss rate and elongation-loss rate are significant references of the SCC susceptibility. According to the curves, the ultimate tensile strength in primary water is 466 MPa while the value in air is 470 MPa. Also, the elongation of the joint in water environment is 31.2% while the elongation in air condition is 28.8%. The ultimate tensile-loss and elongation-loss of the joint are much small, which reveals that the SCC susceptibility of the laser welded joint is tiny.

3.3.2 Fractography

The fractured surfaces of the tested specimens were analyzed using JSM-7800F SEM. The fractographs of the joints after SSRT in air and in simulated primary water were shown in Fig. 5.

Figure 5a, b show the fractographs under different magnification of the joints after SSRT in air condition. The fractographs of the joint consist of much dimples both in the center and at the rim of surface, which shows definite ductile fracture characteristic.

As shown in Fig. 5c, d, the fractographs of the joint tested in the simulated primary water environment present two kinds of features. The center of fracture surface is covered by deformation dimples and reveals the feature of ductile fracture, while the cleavage platform observed at the rim of the fracture surface presents the feature of brittle fracture. The proportion of cleavage fracture regions in the surface reflected the SCC susceptibility of joints. From the fractographs, the proportion of brittle fracture regions of the joint is much small which means its high resistance to SCC.

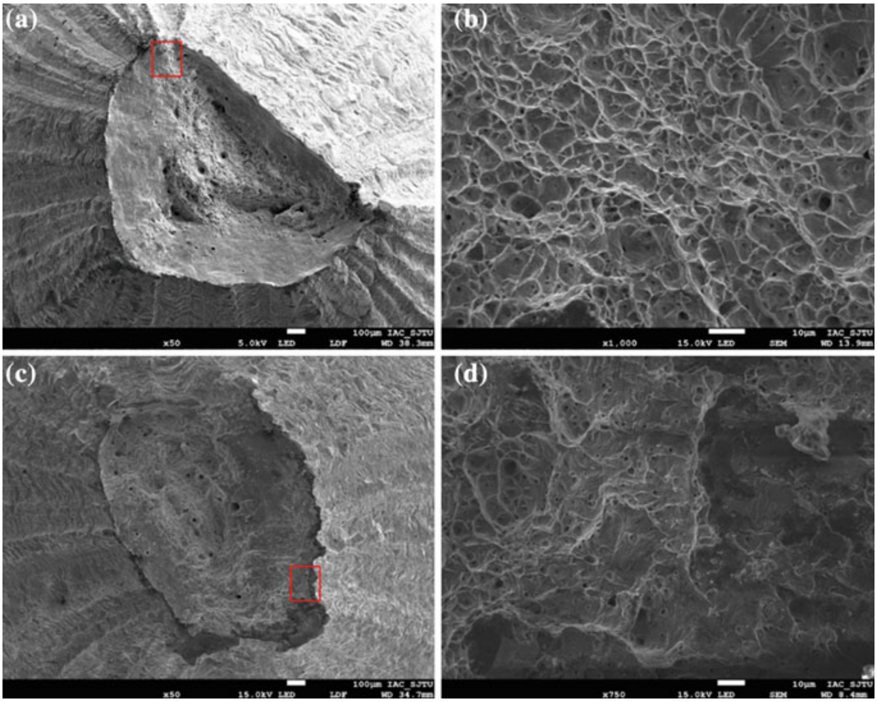

Fig. 5 SEM fractographs of joint in air **a** center area at 50X; **b** edge area at 1000X and in simulated primary water; **c** center area at 50X; **d** edge area at 1000X

4 Conclusion

The microstructure reveals that weld metal is composed of austenitic matrix and δ-ferrite dendrites due to non-equilibrium cooling process. The micro-hardness of the weld metal and HAZ are close to the value of the parent material.

The yield strength and ultimate tensile strength of the joint in simulated primary water are lower than that in air condition. The joint shows good resistance to SCC in simulated primary water environment.

References

1. Subodh K, Shahi AS (2011) Effect of heat input on the microstructure and mechanical properties of gas tungsten arc welded AISI 304 stainless steel joints. Mater Des 32:3617–3623
2. Lee HT, Jeng SL (2001) Characteristics of dissimilar welding of alloy 690 to 304L stainless steel. Sci Technol Weld Joining 6:225–234

3. Jamshidi AH, Farzadi A, Serajzadeh S et al (2009) Theoretical and experimental study of microstructures and weld pool geometry during GTAW of 304 stainless steel. Int J Adv Manufact Technol 42:1043–1051
4. Wolfgang R, Mary PN, George SG (2011) Civilian nuclear accidents. Encycl Inorg Bioinorg Chem 15:1–14
5. Jinya K (2007) Crack growth analysis of SCC under various residual stress distributions near the piping butt-welding. In: ASME Pressure vessels and piping division conference, vol 1, pp 22–26
6. Scott PM (2007) An overview of materials degradation by stress corrosion in PWRs. Eur Fed Corros Publ 1:3–24
7. Takumi T, Katsuhiko F, Koji A (2005) Microstructural characterization of SCC crack tip and oxide film for SUS 316 stainless steel in simulated PWR primary water at 320 °C. J Nucl Sci Technol 42:225–232
8. MacDonald DD, Urquidi-MacDonald M (1991) A coupled environment model for stress corrosion cracking in sensitized type 304 stainless steel in LWR environments. Corros Sci 32:51–81
9. Xu JJ, Chen JY, Duan Y et al (2017) Comparison of residual stress induced by TIG and LBW in girth weld of AISI 304 stainless steel pipes. J Mater Process Technol 248:178–184
10. Muthupandi V, Bala SP, Seshadri SK et al (2003) Effect of weld metal chemistry and heat input on the structure and properties of duplex stainless-steel welds. Mater Sci Eng A 358:9–16